FULL PAPER

Dalton
www.rsc.org/dalton

Electrochemical and theoretical study of the redox properties of transition metal complexes with $\{Pt_2S_2\}$ cores

Rubén Mas-Ballesté,[a] Mercé Capdevila,[a] Pilar González-Duarte,*[a] Mohamed Hamidi,[a,b] Agustí Lledós,[a] Claire Mégret[a] and Dominique de Montauzon†[c]

[a] *Departament de Química, Universitat Autònoma de Barcelona, E-08193 Bellaterra, Barcelona, Spain. E-mail: Pilar.Gonzalez.Duarte@uab.es agusti@klingon.uab.es; Fax: (+34)935811363; Tel: (+34)935813101*

[b] *Département de Chimie, Faculté des Sciences et Techniques, Université Moulay Ismaïl, P.B. 509, Er-Rachidia, Morocco*

[c] *Laboratoire de Chimie de Coordination du CNRS, 205 Route de Narbone, 31077 Toulouse Cedex 4, France*

Received 1st December 2003, Accepted 30th January 2004
First published as an Advance Article on the web 9th February 2004

The oxidation processes undergone by the $\{Pt_2(\mu\text{-}S)_2\}$ core in $[Pt_2(P\cap P)_2(\mu\text{-}S)_2]$ ($P\cap P = Ph_2P(CH_2)_nPPh_2$, $n = 2,3$) complexes have been analysed on the basis of electrochemical measurements. The experimental results are indicative of two consecutive monoelectronic oxidations after which the $\{Pt_2(\mu\text{-}S)_2\}$ core evolves into $\{Pt_2(\mu\text{-}S_2)\}^{2+}$, containing a bridging disulfide ligand. However, the instability of the monoxidised $[Pt_2(P\cap P)_2(\mu\text{-}S)_2]^+$ species formed initially, which converts into $[Pt_3(P\cap P)_3(\mu\text{-}S)_2]^{2+}$, hampered the synthesis and characterisation of the mono and dioxidised species. These drawbacks have been surpassed by means of DFT calculations which have also allowed the elucidation of the structural features of the species obtained from the oxidation of $[Pt_2(P\cap P)_2(\mu\text{-}S)_2]$ compounds. The calculated redox potentials corresponding to the oxidation processes are consistent with the experimental data obtained. In addition, calculations on the thermodynamics of possible processes following the degradation of $[Pt_2(P\cap P)_2(\mu\text{-}S)_2]^+$ are fully consistent with the concomitant formation of monometallic $[Pt(P\cap P)S_2)]$ and trimetallic $[Pt_3(P\cap P)_3(\mu\text{-}S)_2]^{2+}$ compounds. Extension of the theoretical study on the $\{Pt_2Te_2\}$ core and comparisons with the results obtained for $\{Pt_2S_2\}$ have given a more general picture of the behaviour of $\{Pt_2X_2\}$ (X = chalcogenide) cores subject to oxidation processes.

Introduction

The redox chemistry of bimetallic complexes containing a $\{M_2X_2\}$ (X = O,S) core has attracted great interest due to the relevance of these bimetallic complexes in essential biological redox processes such as electron transport[1] or oxygen activation.[2,3] For this reason compounds containing $\{Cu_2O_2\}$,[4] $\{Mn_2O_2\}$,[5] $\{Fe_2O_2\}$,[6] $\{Cu_2S_2\}$,[7] $\{Mn_2S_2\}$[8] or $\{Fe_2S_2\}$[9] cores have been extensively investigated. Often, redox processes involving the $\{M_2X_2\}$ ring provoke significant structural changes as a result of bond-breaking or bond-forming across the ring.

From theoretical analysis it has been established that bonding between antipodal atoms in binuclear complexes obeys qualitative rules based on the occupation of framework molecular orbitals.[10,11] The absence of a through-ring bond is found for eight framework electrons, corresponding to four M–X bonds, whereas the presence of X–X or M–M bonding is anticipated for less than eight framework electrons. From these rules, it can be deduced that an electrochemical oxidation of a $\{M_2X_2\}$ (M = d^8-metal) core induces formation of X–X or M–M bonds by changing the number of electrons in the framework molecular orbitals. Indeed, both M–M and X–X bond forming have been observed upon oxidation of $\{Pt_2X_2\}$ rings. Thus, chemical oxidation of $[NBu_4]_2[Pt_2(\mu\text{-}PPh_2)_2(C_6F_5)_4]$ results in a considerable decrease in the Pt–Pt distance (from 3.621 Å to 2.724 Å) in accordance with the formation of the binuclear Pt(III) compound with a Pt–Pt bond.[12] Analogously, chemical oxidation of $[Pt_2(PEt)_3)_4(\mu\text{-}Te)_2]$ causes a decrease in the Te–Te distance from a nonbonding length (3.263 Å) to a bonding length (2.695 Å), indicating the formation of a Te–Te bond in the dication.[13]

Significant advances in the chemistry of $[L_2Pt(\mu\text{-}S)_2PtL_2]$ complexes have been made in recent years. The ability to bridge sulfide ligands in the $\{Pt_2S_2\}$ core to act as electron-donors accounts for the unusual richness of the chemistry shown by $[L_2Pt(\mu\text{-}S)_2PtL_2]$ complexes.[14] This feature has allowed the synthesis of a wide range of homo- and heterometallic sulfide-bridged aggregates where compounds containing the $\{Pt_2S_2\}$ fragment play the role of metalloligand.[15] Recently, efforts have been focused on understanding the reactivity of $[L_2Pt(\mu\text{-}S)_2PtL_2]$ (L_2 = chelating diphosphine) towards non-metallic electron-acceptor species such as CH_2Cl_2[16] or the simplest electron-acceptor species, *i.e.* the proton.[17] These reactivities, that involve disintegration of the $\{Pt_2S_2\}$ core, consist in multi-step chemical processes that depend on the nature of the terminal phosphine ligand. Only recently has there been interest in studying the catalytic potential of such complexes in organic transformations.[18] However, the redox chemistry of $[L_2Pt(\mu\text{-}S)_2PtL_2]$ complexes still remains almost unexplored. The only available data refers to trimetallic aggregates. Electrochemical studies of the trimetallic clusters $[Pt_3S_2(P\cap P)_3]^{2+}$ ($P\cap P$ = dppm, dppe, dppp, dppb) have shown that the cyclic voltammograms depend on the chelate ring size and that the reversibility of the redox processes varies in the order dppe>dppp>dppb = dppm.[19] In addition, the role of the sulfide ligand in monoelectronic electrochemical oxidation of the $\{Pt_2S_2Hg\}$ core has been demonstrated recently.[20]

In this work the energetic and structural consequences of the successive removal of two electrons from the $\{Pt_2S_2\}$ core will be studied for the complexes $[Pt_2(P\cap P)_2(\mu\text{-}S)_2]$ ($P\cap P$ = 1,2-bis(diphenylphosphino)ethane (dppe) **1**, and 1,3-bis(diphenylphosphino)propane (dppp) **2**, by combining electrochemical measurements and DFT calculations. The structural assignment of the cyclic voltammogram peaks will rely on theoretical calculations, which have recently shown to be very useful for

† Dominique de Montauzon passed away on August 13th, 2001.

DOI: 10.1039/b315509a

studying the redox properties of bimetallic complexes.[21] To asses the validity of our results, and also to extend the scope of this work, a theoretical study of the redox processes in the experimentally studied[13] $[Pt_2(PEt)_3)_4(\mu\text{-}Te)_2]$ (complex **3**) has also been undertaken.

Experimental

Electrochemical measurements

Complexes **1** and **2** were obtained according to published procedures.[16,22] Cyclic voltammograms and controlled potential coulometries of solutions of **1** and **2** in acetonitrile were recorded at 293 ± 1 K in a homemade potentiostat interfaced with a microcomputer. The former were recorded in 2 mmol L^{-1} with platinum wires as the working and counter electrodes. The latter were recorded in a 0.4 mmol L^{-1} solution with a gold disk (125 μm of diameter) and a platinum wire as the working and counter electrodes, respectively. Throughout all the electrochemical measurements NBu_4BF_4 (0.1 mol L^{-1}) was used as the supporting electrolyte and the saturated calomel electrode as the reference electrode. All potentials are reported as reduction potentials with respect to this electrode.

EPR measurements of a 20 mmol L^{-1} solution of **2** in THF were carried out at 230 K in a Bruker ER 200D-SRC spectrometer in parallel with the controlled potential coulometry at 70 mV, using a glassy carbon rod and a platinum wire as the working and counter electrodes, respectively.

Computational details

Calculations were performed with the GAUSSIAN 98 series of programs.[23] Density functional theory (DFT) was applied with the B3LYP functional.[24] Effective core potentials (ECP) were used to represent the innermost electrons of the platinum atom[25a] as well as the electron core of P, S and Te atoms.[25b] The basis set for Pt was that associated with the pseudopotential, with a standard double-ζ LANL2DZ contraction.[23] The basis set for the P S and Te atoms was that associated with the pseudopotential, with a standard double-ζ LANL2DZ contraction[23] supplemented with a set of d-polarization functions.[26] A 6-31G basis set was used for the C and H atoms.[27] Solvent effects were taken into account by means of PCM calculations[28] using standard options of PCM and cavity keywords.[23] Free solvation energies were calculated with CH_2Cl_2 ($\varepsilon = 8.93$) or CH_3CN ($\varepsilon = 36.64$) as the solvent, keeping the geometry optimised for the isolated species (single-point calculations).

Results and discussion

Experimental study of the electrochemical behaviour of $[Pt(dppe)_2(\mu\text{-}S)_2]$(1) and $[Pt(dppp)_2(\mu\text{-}S)_2]$(2) complexes

In order to investigate the oxidation processes of complexes **1** and **2**, electrochemical studies were carried out. Numerical data corresponding to the cyclic voltammograms (CV) recorded on a positive scan at 100 mV s^{-1} are summarised in Table 1. All potentials are reported with respect to the saturated calomel electrode (SCE).

The CV of **1** displays two oxidation waves, at 960 and 56 mV, the former quasi-reversible and the latter irreversible (Fig. 1A). An additional oxidation can be inferred from the quasi-reversible oxidation process at 293 mV. Complex **2** exhibits similar electrochemical behaviour, with two quasi-reversible oxidation waves with peak potentials of 875 and −45 mV (Fig. 1B), whose separation with the corresponding reduction peaks (Table 1) could be indicative of two monoelectronic oxidation processes. In addition, there is a low intensity signal at approximately 200 mV that disappears at higher scan rates. In both complexes, an increase in the scan rate is accompanied

Table 1 Numerical data from cyclic voltammograms of complexes **1** and **2** (4×10^{-4} mol L^{-1}) in acetonitrile containing 0.1 mol L^{-1} NBu_4BF_4 at scan rate of 100 mV s^{-1} at 293 K

	E_{pa}/V	E_{pc}/V	$E_{1/2}$/V	I_a/I_c
$[Pt_2(dppe)_2(\mu\text{-}S)_2]$ (**1**)	0.06	—	0.02	—
	0.29	0.22	0.25	0.87
	0.96	0.85	0.92	0.68
$[Pt_2(dppp)_2(\mu\text{-}S)_2]$ (**2**)	−0.04	−0.12	−0.08	0.69
	0.87	0.77	0.83	0.71

by an increase in the reversibility of the first oxidation wave (E_a = 56 (**1**), −45 (**2**) mV) and a decrease in the intensity of the second wave (E_a = 293 (**1**), $E_a \approx 200$ (**2**) mV). These data give evidence that the oxidation of the $[Pt_2(P\cap P)_2(\mu\text{-}S)_2]$ complexes (**1**, **2**) to yield $[Pt_2(P\cap P)_2(\mu\text{-}S)_2]^+$ (**1**$^+$, **2**$^+$) is followed by decomposition, one of the new species formed being responsible for the second oxidation wave. The stability of the oxidised $[Pt_2(P\cap P)_2(\mu\text{-}S)_2]^+$ form, which has been evaluated on the basis of the dependence of the reversibility of the oxidation wave (E_a = 56 (**1**), −45 (**2**) mV) with the scan rate,[29] being greater for dppp (mean life time *ca.* 10 s) than for dppe (mean life time *ca.* 0.5 ms).

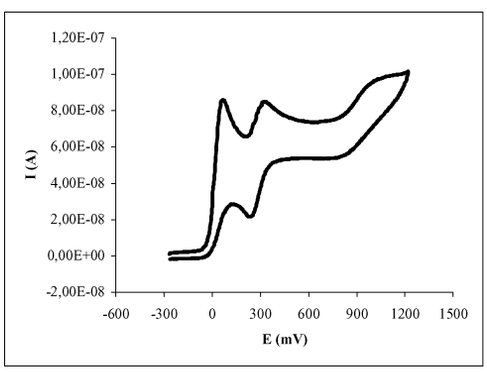

A

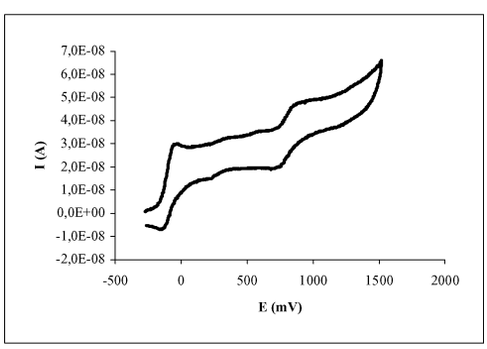

B

Fig. 1 Cyclic voltammograms recorded on a positive scan at a scan rate of 100 mV s^{-1} (4×10^{-4} mol L^{-1} in acetonitrile containing 0.1 mol L^{-1} NBu_4BF_4) at 293 K for complexes **1** (A) and **2** (B).

Controlled-potential coulometry for **1** in acetonitrile at 120 mV as well as for **2** in the same solvent at 70 and 1000 mV indicates that the processes involved are one-electron oxidations. In addition,[31] P NMR spectra of the solutions containing the species obtained by electrolysis of **1** and **2** show the presence of the structurally characterised trinuclear $[Pt_3(P\cap P)_3(\mu_3\text{-}S)_2]^{2+}$ complex, P∩P = dppe,[15e] P∩P = dppp.[17a] This chemical evolution involves, at some stage, the breaking of the $\{Pt_2S_2\}$ central ring in $[Pt_2(P\cap P)_2(\mu\text{-}S)_2]^+$ to give $[Pt_3(P\cap P)_3(\mu_3\text{-}S)_2]^{2+}$. The greater mean life time of $[Pt_2(dppp)_2(\mu\text{-}S)_2]^+$ compared to that of the dppe analogue concords well with previous findings on the dependence of the reactivity of the $\{Pt_2S_2\}$ core in $[Pt_2(P\cap P)_2(\mu\text{-}S)_2]$ metalloligands with the

Table 2 Optimised structural parameters for $[Pt_2(H_2P(CH_2)_nPH_2)_2(\mu\text{-}S)_2]^{z+}$ (n = 2,3; z = 0,1,2). Bond lengths in Å, and angles in degrees[a]

	Pt ⋯ Pt	S ⋯ S	Pt–S	Pt–P	Pt–S–Pt	S–Pt–S	P–Pt–P	θ
1	3.301 *(3.292)*	3.216 *(3.134)*	2.399 *(2.341)*	2.299 *(2.238)*	86.1 *(87.4)*	84.2 *(83.0)*	95.7 *(94.6)*	134.0 *(134.8)*
$\mathbf{1}^{+}$	3.392	2.973	2.387	2.316	90.7	77.1	92.7	130.9
$\mathbf{1}^{2+}$	3.501	2.113	2.457	2.306	90.7	50.3	92.1	104.0
$\mathbf{1}^{2+}{}_{MM}$	2.824	3.811	2.371	2.348	73.1	106.9	85.4	179.8
2	3.286 *(3.235)*	3.228 *(3.101)*	2.406 *(2.332)*	2.293 *(2.255)*	86.9 *(88.9)*	84.1 *(83.6)*	86.5 *(86.2)*	136.0 *(140.2)*
$\mathbf{2}^{+}$	3.401	2.972	2.390	2.313	90.5	77.1	85.6	130.6
$\mathbf{2}^{2+}$	3.505	2.112	2.462	2.306	90.9	50.9	85.64	104.2
$\mathbf{2}^{2+}{}_{MM}$	2.876	3.771	2.381	2.351	74.6	105.3	91.6	176.1

[a] Experimental values in brackets and italic.

diphosphine nature.[16,17] The electrochemical behaviour of **1** and **2** is summarised in Scheme 1, where X denotes the set of products resulting from the decomposition of $[Pt_2(P\cap P)_2(\mu\text{-}S)_2]^{+}$. X and X^{+} include the corresponding trinuclear $[Pt_3(P\cap P)_3(\mu_3\text{-}S)_2]^{2+}$ complex. This easy decomposition hampered the synthesis of $[Pt_2(P\cap P)_2(\mu\text{-}S_2)]^{2+}$ ($\mathbf{1}^{2+}$, $\mathbf{2}^{2+}$) via chemical oxidation of $[Pt_2(P\cap P)_2(\mu\text{-}S)_2]$.

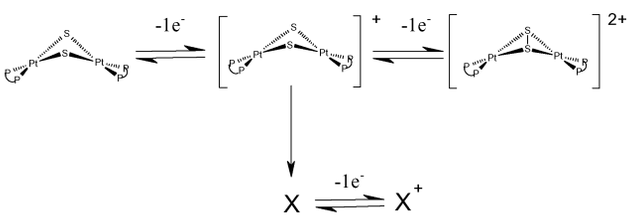

Scheme 1

In order to corroborate that the oxidation of **1** and **2** mainly affects the electronic density around the sulfur atoms, EPR measurements of **2** were run in parallel with the controlled potential coulometry at 70 mV (*vs* SCE) and 230 K. The EPR measurements show clearly that the spectrum of the oxidized $[Pt_2(dppp)_2(\mu\text{-}S)_2]^{+}$ species consists of only one singlet (3370G, g = 2.006). The absence of coupling with neighbouring nuclei indicates that the unpaired electron in $\mathbf{2}^{+}$ is highly localised in the sulfur atoms, suggesting that the electrochemical oxidation at 70 mV can be attributed to the oxidation of S^{2-} to S^{-} and therefore discounting the involvement of platinum ($Pt^{II} \longrightarrow Pt^{III}$) or phosphorus ($P^{III} \longrightarrow P^{IV}$) in the oxidation process. In the case of **1** no EPR signals were recorded in the analogous experiment, probably due to the ease of decomposition of the oxidised $[Pt_2(dppe)_2(\mu\text{-}S)_2]^{+}$ complex to yield diamagnetic species.

Theoretical study of the redox behaviour of $[Pt(P\cap P)_2(\mu\text{-}S)_2]$ ($P\cap P$ = dppe or dppp) complexes

Experimental evidences from circular voltammetry and EPR measurements show that the reversible oxidation of $[Pt_2(P\cap P)_2(\mu\text{-}S)_2]$ ($P\cap P$ = dppe or dppp) complexes results in the abstraction of two electrons from the bridging sulfide ligands. However, the easy disintegration of the bimetallic $\{Pt_2S_2\}$ core in the monocationic $[Pt_2(P\cap P)_2(\mu\text{-}S)_2]^{+}$ species, yielding the trimetallic $[Pt_3(P\cap P)_3(\mu_3\text{-}S)_2]^{2+}$ compound, makes it impossible to isolate and characterise the mono- or dicationic oxidised products. The experimental difficulty of characterising the bimetallic oxidised species has been overcome by means of DFT calculations. The study of molecular and electronic structures of the species involved in the redox process has been completed by the theoretical calculation of their redox potentials. Comparisons between experimental and calculated values of redox potentials can be used as criterion to determine the agreement of theoretical results with experimental data. In addition, this theoretical work includes a thermodynamic assessment of the decomposition reaction of $[Pt_2(P\cap P)_2(\mu\text{-}S)_2]^{+}$ to yield $[Pt_3(P\cap P)_3(\mu_3\text{-}S)_2]^{2+}$. Also, in order to widen the scope of this work towards a more general knowledge about the redox properties of $\{Pt_2X_2\}$ (X = chalcogenide) rings, the theoretical study has been extended to $\{Pt_2Te_2\}$ compounds for which experimental data of their redox behaviour is known.

Molecular and electronic structures

The geometries of the $[Pt_2(P\cap P)_2(\mu\text{-}S)_2]^{n+}$ (n = 0,1,2; $P\cap P$ = dppp or dppe) compounds have been optimised by modelling dppe and dppp real ligands with $H_2P(CH_2)_2PH_2$ (dhpe) or $H_2P(CH_2)_3PH_2$ (dhpp), respectively. The main geometric parameters obtained are given in Table 2. The optimised geometries of the neutral and oxidised forms of the $P\cap P$ = dhpp complex are presented in Fig. 2.

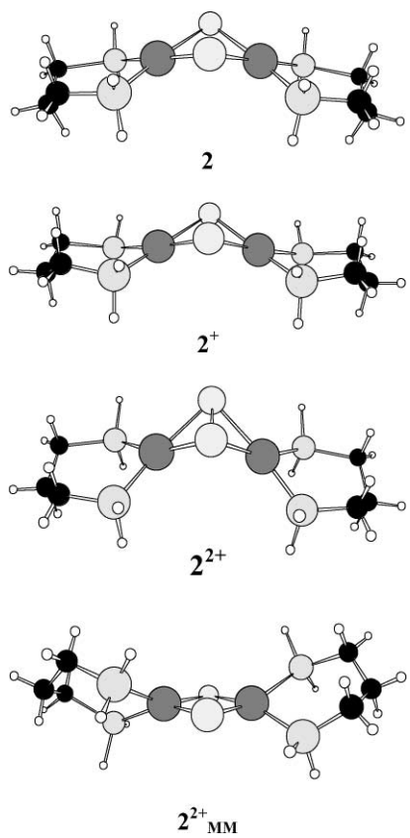

Fig. 2 Optimised structures for neutral and oxidised forms of $[Pt_2(H_2P(CH_2)_3PH_2)_2(\mu\text{-}S)_2]$.

The B3LYP calculated geometries of neutral $[Pt_2(P\cap P)_2(\mu\text{-}S)_2]$ ($P\cap P$ = dhpe or dhpp) compounds have already been reported,[17a] and match well with the X-ray structures of **1**[22] and **2**.[16] Structural trends in edge-sharing binuclear d^8 complexes with $\{M_2(\mu\text{-}X)_2\}$ cores have recently been analysed.[30] A characteristic structural parameter for these complexes is the flexible dihedral angle between the two MX_2 planes (θ) that describes the degree of folding of the M_2X_2 ring. Neutral $[Pt_2(P\cap P)_2$-

(μ-S)$_2$] complexes have a hinged {Pt_2S_2} core ($\theta \simeq 135°$) (Fig. 2). The values of the Pt ··· Pt and S ··· S distances clearly indicate the non-existence of through-ring bonds (see Table 2). Despite the structure of the {Pt_2S_2} core being essentially preserved by the abstraction of one electron from the neutral compounds, some significant structural changes accompany the oxidation process. The main changes when going from **1** and **2** to the monocations $\mathbf{1}^+$ and $\mathbf{2}^+$ are: a slight decrease of the S ··· S distances and S–Pt–S angles, and the lengthening of the Pt ··· Pt distances. With these changes the central ring is squeezed, in such a way that the sulfur atoms approach each other, and the process can be interpreted as the formation of an incipient S–S bond. The structures of $\mathbf{1}^+$ and $\mathbf{2}^+$ described above have been obtained starting from the fully optimised neutral geometries and defining a positive charge for the system. We have looked for alternative structures of the monoxidised species, starting the optimisation from the two geometries of the dications (see below). In all the cases the optimisation has converged to the same geometry, thus confirming that $\mathbf{1}^+$ and $\mathbf{2}^+$ are the only stable structures for the $[Pt_2(P\cap P)_2(\mu\text{-}S)_2]^+$ species. The abstraction of a second electron from the {Pt_2S_2} core enhances the structural tendencies found in the monoxidised complexes, with major consequences in the {Pt_2S_2} ring: a S–S bond is formed (S–S = 2.113 Å in $\mathbf{1}^{2+}$ and S–S = 2.112 in $\mathbf{2}^{2+}$), with the concomitant lengthening of the Pt ··· Pt distance (Pt ··· Pt *ca.* 3.50 Å) and closing of the S–Pt–S angle. Another major change in the {Pt_2S_2} framework upon oxidation is a large folding of the two PtS_2 planes along the S–S axis to give a highly bent geometry ($\theta = 104°$ in $\mathbf{1}^{2+}$ and $\mathbf{2}^{2+}$). Thus, the dicationic species consist in a disulfide S_2^{2-} ligand bridging the two metallic centres, with a very hinged {Pt_2S_2} ring (Fig. 2). The same structural trends were found in the X-ray structure of the $[Pt_2(PEt)_3)_4(\mu\text{-}Te)_2]^{2+}$ complex.[13] A Hartree–Fock calculation of the $[Pt_2(PH_3)_4(\mu\text{-}Se)_2]^{n+}$ (n = 0,2) complex also pointed out the formation of a Se–Se bond with the oxidation.[31]

We have considered the possible existence of isomeric forms of the dications, obtained by Pt oxidation. The optimisation of $[Pt_2(P\cap P)_2(\mu\text{-}S)_2]^+$ starting from a geometry with a short Pt–Pt distance leads to two new minima ($\mathbf{1}^{2+}_{MM}$ and $\mathbf{2}^{2+}_{MM}$) characterised by short Pt–Pt distances (Pt–Pt = 2.824 Å in $\mathbf{1}^{2+}_{MM}$ and Pt–Pt = 2.876 in $\mathbf{2}^{2+}_{MM}$), and long S ··· S distances (> 3.8 Å). These species present a planar {Pt_2S_2} core (θ *ca.* 180°) and coordination geometry around the platinum atoms halfway between square-planar and tetrahedral (P–Pt–P–S dihedral angles of about 160°) (Fig. 2). The same Pt–Pt distance has been found in the B3LYP optimised geometry of the oxidised $[Pt_2(C_6F_5)_4(\mu\text{-}PH_2)_2]$, calculated as a model of $[Pt_2(C_6F_5)_4(\mu\text{-}PPh_2)_2]$ and described as a Pt(III)-Pt(III) compound.[12b] The structural data of $\mathbf{1}^{2+}_{MM}$ and $\mathbf{2}^{2+}_{MM}$ indicates the oxidation of the metallic centres and the resulting formation of a Pt–Pt bond. However the products of the metal oxidation lie more than 140 kJ mol^{-1} above those of the sulfide oxidation (147.9 kJ mol^{-1} for $\mathbf{1}^{2+}_{MM}$ and 151.4 kJ mol^{-1} for $\mathbf{2}^{2+}_{MM}$). The greater stability of the disulfide containing $[Pt_2(P\cap P)_2(\mu\text{-}S_2)]^{2+}$ complexes suggests that this isomer is the final product for the abstraction of two electrons from the neutral $[Pt_2(dppp)_2(\mu\text{-}S)_2]$ compound. This hypothesis will be confirmed by the comparison of the calculated and experimental redox potentials (see below).

Fig. 3 shows 3-D plots of the $[Pt_2(dhpp)_2(\mu\text{-}S)_2]^{n+}$ (n = 0,1,2) orbitals directly involved in the redox process. The HOMO of the neutral $[Pt_2(dhpp)_2(\mu\text{-}S)_2]$ complex consists in an antibonding combination of p_π orbitals of the sulfur atoms perpendicular to the {Pt_2S_2} core (p_z). The semi-occupied molecular orbital (SOMO) of the monocationic species is essentially the same combination of p_π orbitals, localised in the S atoms in agreement with the EPR measurements. Thus, it is clear that the electron is removed from the non-bonding electron pairs in the p_π orbitals of sulfide ligands. The structural

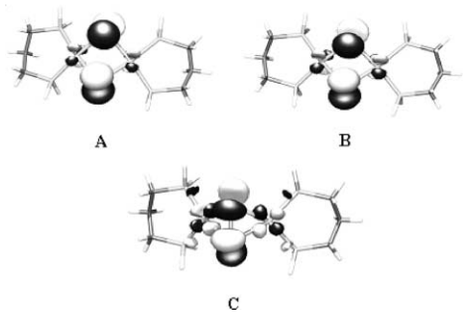

Fig. 3 HOMO (A), SOMO (B) and LUMO (B) of $[Pt_2(dhpp)_2(\mu\text{-}S)_2]$ $[Pt_2(dhpp)_2(\mu\text{-}S)_2]^+$ and $[Pt_2(dhpp)_2(\mu\text{-}S_2)]^{2+}$.

changes, as a consequence of the oxidation of the {Pt_2S_2} core, provoke an increase in the participation of d orbitals of the metallic centre and an increased contribution of sulfur p_y orbitals in the LUMO of the dication. This qualitative orbital analysis shows that the molecular orbitals implied in the electrochemical oxidation of the complexes studied correspond to the sulfide ligands. The redox behaviour of the sulfide ligands in $[Pt_2(P\cap P)_2(\mu\text{-}S)_2]$ complexes is in strong accordance with the widely reported nucleophilicity of the bridging sulfur atoms of complexes containing a {Pt_2S_2} core.[14–18]

The evolution of NPA (natural population analysis) charges throughout the oxidation process gives an indication of how the positive charge is distributed. The atomic charges in the neutral $[Pt_2(dhpe)_2(\mu\text{-}S)_2]$ complex are $-0.66e$, $+0.11e$ and $+0.56e$, for the S, Pt and P atoms, respectively. In the monooxidised $\mathbf{1}^+$ the negative charge on each sulfur atom has decreased by $0.27e$, whereas the positive charges in Pt and P atoms have only increased by $0.01e$. In $\mathbf{1}^{2+}$ the atomic charges in each S, Pt and P atom are $-0.11e$, $+0.11e$ and $+0.60e$. The remainder of the positive charge goes to the H atoms of the P–P ligands. A very similar evolution of the atomic charges is found in the $[Pt_2(dhpp)_2(\mu\text{-}S)_2]$ system. So the NPA charges are fully consistent with the oxidation of the sulfur ligands. It is worth mentioning that in the $\mathbf{1}^{2+}_{MM}$ isomer the positive charge increases in the platinum centre in accordance with the fact that the oxidation takes place in metal atoms.

Redox potentials

The theoretical data reported above indicates that the electrochemical oxidation of $[Pt(P\cap P)_2(\mu\text{-}S)_2]$ binuclear complexes results in the oxidation of sulfide ligands in the {Pt_2S_2} core yielding the disulfide containing $[Pt(P\cap P)_2(\mu\text{-}S_2)]^{2+}$ products. However, the main experimental data obtained in this work are the potentials of electrochemical oxidation, which remain at this point without a theoretical estimation. Thus, with the aim of verifying that the theoretical and experimental data are fully consistent, the redox potentials of the oxidation processes have been calculated.

In order to obtain realistic reaction energies of processes where charged species are generated, is necessary to take into account the solvent effects. With this aim we have calculated the Gibbs energy changes, (ΔG_{ox}) for the oxidation reactions in acetonitrile, following the approach based on continuum solvent models that can be found in recent literature.[21,32] An accurate calculation of the redox potentials is a very demanding problem. Only very recently has it been possible to calculate reduction potentials for the cyclooctatetraene and nitrobenze that are highly consistent with the experimental values.[33] We are aware of the difficulties of such calculations in large systems, with transition metal atoms, and that only semi-quantitative results can be expected. From the $(\Delta G_{ox})_{sol}$, the absolute redox potential can be calculated according to the following expression:

$$E_{ox} = (\Delta G_{ox})_{sol}/nF$$

Table 3 Calculated and experimental electrochemical potentials for the oxidation of $[Pt_2(P\cap P)_2(\mu\text{-}S)_2]$ complexes

P∩P			$(\Delta G_{ox})_{sol}$/ kJ mol^{-1}	Calculated absolute potential/V	Calculated potential *vs.* SCE/V	Experimental redox potential/V
$H_2P(CH_2)_2PH_2$	$M\longrightarrow M^+$		+430.9	4.47	−0.20	+0.02
	$M^+\longrightarrow M^{2+}$	$\mathbf{1}^{2+}$	+507.0	5.26	+0.59	+0.92
		$\mathbf{1}^{2+}{}_{MM}$	+636.2	6.60	+1.93	
$H_2P(CH_2)_3PH_2$	$M\longrightarrow M^+$		+428.8	4.45	−0.22	−0.08
	$M^+\longrightarrow M^{2+}$	$\mathbf{2}^{2+}$	+504.9	5.24	+0.57	+0.83
		$\mathbf{2}^{2+}{}_{MM}$	+637.8	6.62	+1.95	

Experimental data are always reported relative to a reference electrode. To obtain the values referenced with respect to the potential of the saturated calomel electrode (SCE) it is necessary to calculate the difference between the absolute potential obtained from the considered complex and the absolute potential of the reference electrode. The value of the absolute reduction potential of the hydrogen electrode appears in literature as +4.43 V.[34] From this value, and considering that the well-known reduction potential of SCE with respect to the hydrogen electrode is +0.24 V, the values of the potentials of the studied complexes, taking the SCE as a reference, can be calculated. The calculated redox potentials are given in Table 3. Despite these kinds of calculations only having semi-quantitative significance, the accordance between the experimental and theoretical values is remarkable. The experimental differences between the redox potentials corresponding to the first and second oxidations are 0.90 V in **1** and 0.91 V in **2**. The calculated differences in the theoretical models of **1** and **2** are both 0.79 V. Depending on the considered isomer of the dicationic species two different values of the redox potential are obtained for the process $M^+\longrightarrow M^{2+}$. However, while the calculated values corresponding to the process of obtaining the most stable isomers ($\mathbf{1}^{2+}$ and $\mathbf{2}^{2+}$) are close to the experimental redox potentials, the values for the $\mathbf{1}^{2+}{}_{MM}$ and $\mathbf{2}^{2+}{}_{MM}$ isomers are in marked disaccord with the experimental data. The closeness between the electrochemical data and DFT calculations confirms that the experimentally observed abstraction of two electrons from $[Pt_2(P\cap P)_2(\mu\text{-}S_2)]$ results in the formation of the disulfide containing complexes $[Pt_2(P\cap P)_2(\mu\text{-}S_2)]^{2+}$.

Reaction of degradation of monocationic complexes

According to the CV data, the experimental difficulty to determine all species implied in the oxidation of the $\{Pt_2S_2\}$ core arises from the disintegration of the monocationic species. Thus, both experiments of electrochemical or chemical oxidation have as a result the formation of several species, the main product being the well-known trimetallic $[Pt_3(P\cap P)_3(\mu_3\text{-}S)_2]^{2+}$,[15e,17a] compounds. Probably, the evolution of the system is the result of a complex process where kinetic and thermodynamic factors have an important role. However, to get some ideas on how the disintegration of the monocationic complexes can proceed, we have considered several pathways for the degradation of the bimetallic monocationic species. In order to study the thermodynamic viability of the processes in acetonitrile as the solvent, single point PCM calculations on the optimised structures were performed and their ΔG in acetonitrile were calculated. We do not consider the kinetics of these processes, which probably include several steps. Notwithstanding, a thermodynamic estimation of the disintegration processes can give an additional insight into the chemical systems presented here.

The first reaction considered is the recombination of two monocations to give the trimetallic complexes and a neutral mononuclear complex:

$$2\,[Pt_2(P\cap P)_2(\mu\text{-}S)_2]^+\longrightarrow [Pt_3(P\cap P)_3(\mu_3\text{-}S)_2]^{2+} + [Pt(P\cap P)(S_2)] \quad (1)$$

For both the complexes considered this reaction appears as very favourable, with ΔG values of −41.8 kJ per mol of $[Pt_2(dhpe)_2(\mu\text{-}S)_2]^+$ and −45.1 kJ per mol of $[Pt_2(dhpp)_2(\mu\text{-}S)_2]^+$. We have calculated the redox potentials for the oxidation of the mononuclear product of reaction 1:

$$[Pt(P\cap P)S_2)] \longrightarrow [Pt(P\cap P)(S_2)]^+$$

The calculated redox potentials, with reference to the SCE, are 0.16 V and 0.13V, for P∩P = dhpe and dhpp, respectively. During the CV experiments we measured an oxidation potential of 0.25V for a disintegration product of $[Pt_2(dppe)_2(\mu\text{-}S)_2]^+$. Comparing the theoretical and experimental values, it is likely that $[Pt(dppe)(S_2)]$ is the detected disintegration product. In the optimised structure of this complex an S–S distance of 2.117 Å and a S–Pt–S angle of 52.2° were found, indicating the presence of a η^2-disulfide ligand. The only example found in literature, recently reported, of a complex structurally characterized containing the $\{PtS_2\}$ ring, shows similar structural features.[35]

We have also calculated the energetics of the reaction:

$$3\,[Pt_2(P\cap P)_2(\mu\text{-}S)_2]^+\longrightarrow 2\,[Pt_3(P\cap P)_3(\mu_3\text{-}S)_2]^{2+} + \tfrac{1}{2}\,S_4{}^{2-} \quad (2)$$

The calculated ΔG in acetonitrile, which are similar for both diphosphine ligands, are indicative that this process is also favoured (ΔG = −19.2 kJ per mol of $[Pt_2(dhpe)_2(\mu\text{-}S)_2]^+$ and ΔG = −22.1 kJ per mol of $[Pt_2(dhpp)_2(\mu\text{-}S)_2]^+$), although it is less exothermic than reaction (1). As for reaction (1), we have calculated the redox potential for the oxidation of the reaction product:

$$S_4{}^{2-}\longrightarrow S_4{}^-$$

Comparison of the value obtained (−2.52V) with the measured oxidation potential of the disintegration product (0.25V) led us to discard the $S_4{}^{2-}$ anion as the CV detected species from the degradation of the monocationic species. Thus, from the theoretical results it is reasonable to conclude that reaction (1) is, probably, the source of the experimental difficulty to characterise the oxidised forms of the $\{Pt_2S_2\}$ compounds. It must be pointed out that despite the experimentally observed different stabilities of the monocationic species depending on the terminal diphosphine ligand, no thermodynamic differentiation is found by DFT calculations. This fact can be attributed to kinetic reasons that have already been reported in the literature for the formation of the trimetallic species from the reaction of $\{Pt_2S_2\}$ compounds with protic acids.[17a]

Comparison with telluride analogues

4The closest work, found in literature, to the study presented here consists in the isolation and characterisation of $[Pt_2(PEt_3)_4(\mu\text{-}Te)_2]$ (**3**) and $[Pt_2(PEt)_3)_4(\mu\text{-}Te_2)]^{2+}$ ($\mathbf{3}^{2+}$).[13] Taking advantage of the existence of electrochemical and structural experimental data corresponding to these $\{Pt_2Te_2\}$ compounds, this work has been completed by the theoretical study of the oxidation processes of these complexes. Comparisons between the results obtained for $\{Pt_2Te_2\}$ and $\{Pt_2S_2\}$ complexes can

Table 4 Optimised structural parameters for $[Pt_2(P(CH_3)_3)_4(\mu\text{-}S)_2]^{z+}$ (z = 0,1,2). Bond lengths in Å, and angles in degrees[a]

	Pt ⋯ Pt	Te ⋯ Te	Pt–Te	Pt–P	Pt–Te–Pt	Te–Pt–Te	P–Pt–P	θ
3	4.177 *(4.100)*	3.390 *(3.263)*	2.706 *(2.618)*	2.346*(2.286)*	101.0 *(103.0)*	77.6 *(77.0)*	105.4 *(106.3)*	164.0 *(180.0)*
$\mathbf{3}^{+}$	3.889	3.099	2.705	2.356	94.6	71.5	98.1	129.8
$\mathbf{3}^{2+}$	3.831 *(3.648)*	2.713 *(2.697)*	2.741 *(2.634)*	2.343*(2.273)*	*88.6 (87.5)*	*59.3 (61.5)*	*98.5 (98.3)*	*107.0 (107.4)*

[a] Experimental values for the complex with phosphine = PEt_3 in brackets.

$$[Pt_2(\mu\text{-}Te)_2(P(CH_3)_3)_4] \xrightarrow{-0.73\ V} [Pt_2(\mu\text{-}Te)_2(P(CH_3)_3)_4]^{+} \underset{(+0.40\ V)}{\xrightarrow{+0.23\ V}} [Pt_2(\mu\text{-}Te_2)(P(CH_3)_3)_4]^{2+}$$

Scheme 2

improve the understanding of factors that modulate the redox activity of bimetallic $\{M_2X_2\}$ (X = Chalcogenide) systems.

The structures of neutral, monocationic and dicationic $\{Pt_2Te_2\}$ species have been optimised by taking PMe_3 as the terminal ligand. The main optimised geometrical parameters are given in Table 4, together with the X-ray determined values for **3** and $\mathbf{3}^{2+}$.[13] The structure of the monooxidised species has never been reported. The B3LYP structures of $[Pt_2(PMe)_4(\mu\text{-}Te)_2]$ and $[Pt_2(PMe)_3)_4(\mu\text{-}Te_2)]^{2+}$ are highly consistent with their experimental analogues. The neutral compound has a flat $\{Pt_2Te_2\}$ central ring without through-ring bonds (Te ⋯ Te = 3.390 Å) according with the X-ray structures published for the compounds containing $\{M_2Te_2\}$ (M = Pd,Pt) cores.[13,36] The removal of one electron causes the hinging of the $\{Pt_2Te_2\}$ core (θ = 129.8°) and the incipient formation of a Te–Te bond (Te ⋯ Te = 3.099 Å). The removal of the second electron essentially results in the enhancement of the folding of the core (θ = 107.0°) and the complete formation of the Te–Te bond (Te ⋯ Te = 2.713 Å). Therefore, a bridging ditelluride is present in the dication. We have also looked for a $\mathbf{3}^{2+}_{MM}$ isomer, with a short Pt–Pt distance. However in this case only the isomer of the dicationic complex with a short Te–Te distance was found.

The orbital analysis of the $\{Pt_2Te_2\}$ compounds gives the same qualitative results as the previous study of sulfide analogues: the molecular orbitals involved in the oxidation of bimetallic $\{Pt_2X_2\}$(X = Chalcogenide) species correspond to the chalcogenide anion. The energy of the HOMO of $[Pt_2(PMe_3)_4(\mu\text{-}Te)_2]$ (−3.46eV) is approximately 0.43 eV above the HOMO of the $[Pt_2(\mu\text{-}S)_2(P\cap P)_2]$ complexes. This fact is in strong accordance with the lower electronegativity of tellurium compared with that of sulfur and indicates that the lone electron-pairs in chalcogenide anions are more accessible in $\{Pt_2Te_2\}$ compounds than in their sulfide-containing analogues. This effect is also observed in the calculated values of redox potentials. The evolution of the NPA charges throughout the oxidation is consistent with the process taking place in the telluride ligands. Charges on each Te atom are −0.49e, −0.18e and +0.06e, in the neutral, monocationic and dicationic complexes, respectively.

In order to obtain the redox potentials and the ΔG of the degradation process of the monocationic species, single point PCM calculations in CH_2Cl_2 (the solvent used in the experiments reported in literature) were performed. The calculated redox potentials are presented in the Latimer diagram shown in Scheme 2. The results obtained show that **3** exhibits two monoelectronic oxidations. Our value of the redox potential for the second monooxidation (+0.22 V) is not far from that of the irreversible oxidation wave measured for $[Pt_2(PEt_3)_4(\mu\text{-}Te)_2]$ (+0.40 V).[13] The calculated difference between the potential values corresponding to the first and second electrochemical oxidations of **3** (0.96 V) is comparable to that observed in the study of $\{Pt_2S_2\}$ compounds. Nevertheless, the values of redox potentials found for $\{Pt_2Te_2\}$ complexes are significantly lower than those observed for compounds containing $\{Pt_2S_2\}$. This observation is highly consistent with the higher energy of the HOMO of $[Pt_2(PMe_3)_4(\mu\text{-}Te)_2]$ complex compared with that of $\{Pt_2S_2\}$ compounds and with the lower electronegativity of the tellurium atom.

The process to obtain the trimetallic complex $[Pt_3(PEt_3)_6(\mu_3\text{-}Te)_2]^{2+}$ accompanying the formation of the oxidised $\mathbf{3}^{2+}$ has been reported.[13] We have also analysed the viability of the formation of the trimetallic complex from the degradation of the monocation, by calculating the energetics of the following reactions in dichloromethane:

$$2\,[Pt_2(PMe_3)_4(\mu\text{-}Te)_2]^{+} \longrightarrow [Pt_3(PMe_3)_6(\mu_3\text{-}Te)_2]^{2+} + [Pt(PMe_3)_2Te_2)] \quad (3)$$

$$3\,[Pt_2(PMe_3)_4(\mu\text{-}Te)_2]^{+} \longrightarrow 2\,[Pt_3(PMe_3)_6(\mu_3\text{-}Te)_2]^{2+} + \tfrac{1}{2}\,Te_4^{2-} \quad (4)$$

These two processes are analogous to reactions (1) and (2) which are considered for the degradation of the $\{Pt_2S_2\}$ monooxidised species in acetonitrile. The theoretical results indicate that reaction (3) is slightly exothermic (−8.3 kJ per mol of $[Pt_2(PMe_3)_4(\mu\text{-}Te)_2]^{+}$) whereas reaction (4) is endothermic (ΔG = +32.2 kJ per mol of $[Pt_2(P(CH_3)_3)_4(\mu\text{-}Te)_2]^{+}$). Matching well with the reported results, the cleavage of $\{Pt_2Te_2\}^{+}$ is significantly less favourable than that of $\{Pt_2S_2\}^{+}$. Consequently, although the formation of $[Pt_3(PEt_3)_6(\mu_3\text{-}Te)_2]^{2+}$ is also a competitive reaction with the process to obtain $\mathbf{3}^{2+}$, it has been possible to isolate and characterise $[Pt_2(PEt_3)_4(\mu\text{-}Te_2)]^{2+}$ in contrast with the results obtained with the $\{Pt_2S_2\}$ compounds.

Concluding remarks

Experimental and theoretical data reported here demonstrate the possibility of $\{Pt_2(\mu\text{-}X)_2\}$ (X = chalcogenide) systems to show reversible redox processes comparable to those observed in several metalloenzymes. The oxidation induces major structural changes in the $\{Pt_2X_2\}$ ring and entails formation of a through-ring X–X bond and a large folding of the two Pt_2X planes along the X–X axis. The oxidised species can be described as containing a bridging dichalcogenide ligand. The reversible oxidation reaction $\{Pt_2(\mu\text{-}X)_2\} \longrightarrow \{Pt_2(\mu\text{-}X_2)\}^{2+}$ appears plausible, considering that, in all cases studied, the potential of this process is less than 1 V (*vs.* SCE). The experimental data reported here also demonstrate that the redox properties of the $\{Pt_2(\mu\text{-}S)_2\}$ are tuneable by means of subtle parameters such as changing the P–Pt–P bite angle caused by replacing dppe by dppp as the terminal ligands.

Nevertheless, the decomposition of monooxidised $\{Pt_2(\mu\text{-}X)_2\}^{+}$ species to yield $\{Pt_3(\mu_3\text{-}X)_2\}^{2+}$ appears as a competitive reaction with the formation of dichalcogenide containing $\{Pt_2(\mu\text{-}X_2)\}^{2+}$ species. Fortunately, as shown in the literature, the ability of bimetallic species $\{Pt_2(\mu\text{-}X)_2\}$ to form trimetallic $\{Pt_3(\mu_3\text{-}S)_2\}^{2+}$ complexes can be tuned by controlling, for example, the nature of terminal ligands. Future works in this field could be addressed to the study of $\{M_2(\mu\text{-}X)_2\}$ complexes where the formation of $\{M_3(\mu_3\text{-}X)_2\}^{2+}$ compounds is disfavoured. The use of bulky terminal ligands preventing the

formation of the dead-end $\{M_3(\mu_3\text{-}X)_2\}^{2+}$ species could be one of the possible strategies.

In conclusion, this work shows that the redox chemistry of $\{M_2(\mu\text{-}X)_2\}$ has the characteristic subtlety found in biological systems, where several electronic and structural parameters play an important role. New insights on the factors that allow control over the redox properties of systems containing biological and synthetic $\{M_2(\mu\text{-}X)_2\}$ seems to be a promising area, which deserves further development.

Acknowledgements

Financial support from the *Ministerio de Ciencia y Tecnología* of Spain (projects BQU2001-1976 and BQU2002-04110-CO2-02) is gratefully acknowledged. RMB is indebted to the *Universitat Autònoma de Barcelona* for a pre-doctoral scholarship. The use of the computational facilities of the Centre de Supercomputació de Catalunya (CESCA) is also gratefully appreciated.

References

1 (*a*) J. W. Peteres, W. N. Lanzilotta, L. Brian and L. Seefeldt, *Science*, 1998, **282**, 1858; (*b*) S. J. Lippard and J. M. Berg, *Principles of Bioinorganic Chemistry*, University Science Books, Mill Valley, CA, 1994.
2 (*a*) G. Aullón E. Ruiz and S. Alvarez, *Chem. Eur. J.*, 2002, **8**, 2508; (*b*) E. I. Solomon, T. C. Brunold, M. I. Davis, J. N. Kemsley, S.-K. Lee, F. Lehnert, F. R. Neese, A. J. Skulan, Y.-S. Yang and J. Zhou, *Chem Rev.*, 2000, **100**, 235; (*c*) J. van der Stubbe and W. A. Donk, *Chem Rev.*, 1998, **98**, 705.
3 L. Que Jr. and W. B. Tollman, *Angew. Chem. Int. Ed. Engl.*, 2002, **41**, 1114.
4 (*a*) S. Itoh, M. Taki, H. Nakao, P. L. Holland, W. B. Tolman, L. Que Jr. and S. Fukuzumi, *Angew. Chem Int. Ed. Engl.*, 2000, **39**, 398; (*b*) J. A. Halfen, S. Mahapatra, E. C. Wilkinson, G. Pan, X. Wang, V. G. Young Jr., L. Que Jr. and W. B. Tolman, *Science*, 1996, **271**, 1397.
5 (*a*) R. Manchada, G. V. Burdvig and R. H. Crabtree, *Coord. Chem. Rev.*, 1995, **144**, 1; (*b*) K. Wieghardt, *Angew. Chem Int. Ed. Engl.*, 1989, **28**, 1153.
6 Y. Zang, Y. Dong, L. Que Jr., K. Kauffmann and E. Münk, *J. Am. Chem. Soc.*, 1995, **117**, 1169.
7 K. Fujisawa, Y. Moro-oka and N. Kitajima, *J. Chem. Soc., Chem. Commun.*, 1994, 623.
8 R. D. Adams, O.-S. Kwon and M. D. Smith, *Inorg. Chem.*, 2002, **41**, 1658.
9 (*a*) N. Ueyama, Y. Yamada, T.-A. Okamura, S. Kimura and A. Nakamura, *Inorg. Chem.*, 1996, **35**, 6475; (*b*) N. Ueyama, S. Ueno, T. Sugawara, K. Tatsumi, N. Nakamura and N. Yasuoka, *J. Chem. Soc., Dalton Trans.*, 1991, 2723; (*c*) A. Salifoglou, M. G. Kanatzidis and D. Coucouvanis, *Inorg. Chem.*, 1988, **27**, 3394.
10 S. Alvarez, A. A. Palacios and G. Aullón, *Coord. Chem. Rev.*, 1999, **185–186**, 431.
11 (*a*) A. A. Palacios, P. Alemany and S. Alvarez, *J. Chem. Soc., Dalton Trans.*, 2002, 2235; (*b*) A. A. Palacios, G. Aullón, P. Alemany and S. Alvarez, *Inorg. Chem.*, 2000, **39**, 3166; (*c*) X.-Y. Liu, A. A. Palacios, J. J. Novoa and S. Alvarez, *Inorg. Chem.*, 1998, **37**, 1202; (*d*) G. Aullón, P. Alemany and S. Alvarez, *J. Organomet. Chem.*, 1994, **478**, 75; (*e*) P. Alemany and S. Alvarez, *Inorg. Chem.*, 1992, **31**, 4266.
12 (*a*) E. Alonso, J. M. Casas, J. Forniés, C. Fortuño, A. Martín, A. G. Orpen, C. A. Tsipis and A. C. Tsipis, *Organometallics*, 2001, **20**, 5571; (*b*) E. Alonso, J. M. Casas, F. A. Cotton, X. Feng, J. Forniés, C. Fortuño and M. Tomas, *Inorg. Chem.*, 1999, **38**, 5034.
13 A. L. Ma, J. B. Thoden and L. F. Dahl, *J. Chem. Soc., Chem. Commun.*, 1992, 1516.
14 S.-W. A. Fong and T. S. A. Hor, *J. Chem. Soc., Dalton Trans.*, 1999, 639 and references therein.
15 Selected recent references: (*a*) S.-W. A. Fong, W. T. Yap, W. Teck, J. J. Vittal, W. Henderson and T. S. A. Hor, *J. Chem. Soc., Dalton Trans.*, 2002, 1826; (*b*) Z. Li, Z.-H. Loh, K. F. Mok and T. S. A. Hor, *Inorg. Chem.*, 2000, **39**, 5299; (*c*) Z. Li, X. Xu, S. Khoo, K. F. Mok and T. S. A. Hor, *J. Chem. Soc., Dalton Trans.*, 2000, 2901; (*d*) H. Liu, C. Jiang, J. S. L. Yeo, K. F. Mok, L. K. Liu, T. S. A. Hor and Y. K. Yan, *J. Organomet. Chem.*, 2000, **595**, 276; (*e*) M. Capdevila, Y. Carrasco, W. Clegg, R. A. Coxall, P. González-Duarte, A. Lledós and J. A. Ramírez, *J. Chem. Soc., Dalton Trans.*, 1999, 3103.
16 R. Mas-Ballesté, M. Capdevila, P. A. Champkin, W. Clegg, R. A. Coxall, A. Lledós, C. Mégret and P. González-Duarte, *Inorg. Chem.*, 2002, **41**, 3218.
17 (*a*) R. Mas-Ballesté, G. Aullón, P. A. Champkin, W. Clegg, C. Megret, P. González-Duarte and A. Lledós, *Chem. Eur. J.*, 2003, **9**, 5023; (*b*) G. Aullón, M. Capdevila, W. Clegg, P. González-Duarte, A. Lledós and R. Mas-Ballesté, *Angew. Chem. Int. Ed. Engl.*, 2002, **41**, 2776.
18 (*a*) S. H. Chong, A. Tjindrawan and T. S. A. Hor, *J. Mol. Cat. A*, 2003, **204**, 267; (*b*) H. Brunner, M. Weber and M. Zabel, *J. Organomet. Chem.*, 2003, **684**, 6.
19 (*a*) K. Matsumoto, K. Takahashi, M. Ikuzawa, H. Kimoto and S. Okeya, *Inorg. Chim. Acta*, 1998, **281**, 174; (*b*) K. Matsumoto, M. Ikuzawa, M. Kamikubo and S. Ooi, *Inorg. Chim. Acta*, 1994, **217**, 129; (*c*) K. Matsumoto, N. Saiga, S. Tanaka and S. Ooi, *J. Chem. soc., Dalton Trans.*, 1991, 1265.
20 X. Xu, S-W. A. Fong, Z. Li, Z.-H. Loh, J. J. Vittal, W. Henderson, S-B. Khoo and T. S. A. Hor, *Inorg. Chem.*, 2002, **41**, 6838.
21 (*a*) S. Blasco, I. Demachy, Y. Jean and A. Lledós, *New J. Chem.*, 2001, **25**, 611; (*b*) M.-H. Baik, T. Ziegler and C. K. Schauer, *J. Am. Chem. Soc.*, 2000, **122**, 9143.
22 M. Capdevila, Y. Carrasco, W. Clegg, P. González-Duarte, A. Lledós, J. Sola and G. Ujaque, *Chem. Commun.*, 1998, 597.
23 M. J. Frisch, G. W. Trucks, H. B. Schlegel, G. E. Scuseria, M. A. Robb, J. R. Cheeseman, V. G. Zakrzewski, J. A. Montgomery, R. E. Stratmann, J. C. Burant, S. Dapprich, J. M. Millam, A. D. Daniels, K. N. Kudin, M. C. Strain, O. Farkas, J. Tomasi, V. Barone, M. Cossi, R. Cammi, B. Mennucci, C. Pomelli, C. Adamo, S. Clifford, J. Ochterski, G. A. Petersson, P. Y. Ayala, Q. Cui, K. Morokuma, D. K. Malick, A. D. Rabuck, K. Raghavachari, J. B. Foresman, J. Cioslowski, J. V. Ortiz, B. B. Stefanov, G. Liu, A. Liashenko, P. Piskorz, I. Komaromi, R. Gomperts, R. L. Martin, D. J. Fox, T. Keith, M. A. Al-Laham, C. Y. Peng, A. Nanayakkara, C. Gonzalez, M. Challacombe, P. M. W. Gill, B. Johnson, W. Chen, M. W. Wong, J. L. Andres, C. Gonzalez, M. Head-Gordon, E. S. Replogle and J. A. Pople, *Gaussian98 (Revision A.7)*; Gaussian Inc.: Pittsburgh, PA, 1998.
24 (*a*) C. Lee, W. Yang and R. G. Parr, *Phys. Rev. B*, 1988, **37**, 785; (*b*) A. D. Becke, *J. Chem. Phys.*, 1993, **98**, 5648; (*c*) P. J. Stephens, F. J. Delvin, C. F. Chabalowski and M. J. Frisch, *J. Phys. Chem.*, 1994, **98**, 11623.
25 (*a*) P. J. Hay and W. R. Wadt, *J. Chem. Phys.*, 1985, **82**, 299; (*b*) W. R. Wadt and P. J. Hay, *J. Chem. Phys.*, 1985, **82**, 284.
26 A. Höllwarth, M. Böhme, S. Dapprich, A. W. Ehlers, A. Gobbi, V. Jonas, K. F. Köhler, R. Stegman, A. Veldkamp and G. Frenking, *Chem. Phys. Lett.*, 1993, **208**, 237.
27 W. J. Hehre, R. Ditchfield and J. Pople, *J. Chem. Phys.*, 1972, **56**, 2257.
28 (*a*) C. Amovilli, V. Barone, R. Cammi, E. Cancès, M. Cossi, B. Mennucci, C. S. Pomelli and J. Tomasi, *Adv. Quantum Chem.*, 1998, **32**, 227; (*b*) J. Tomasi and M. Persico, *Chem. Rev.*, 1994, **94**, 2027.
29 R. S. Nicholson and I. Shain, *Anal. Chem.*, 1964, **36**, 706.
30 G. Aullón, G. Ujaque, A. Lledós and S. Alvarez, *Inorg. Chem.*, 1998, **37**, 804.
31 A. Bencini, M. di Vaira, R. Morassi and P. Stoppioni, *Polyhedron*, 1996, **15**, 2079.
32 (*a*) P. Winget, E. J. Weber, C. J. Cramer and D. G. Truhlar, *Phys. Chem. Chem. Phys.*, 2000, **2**, 1231; (*b*) L. J. Kette, S. P. Bates and A. R. Mount, *Phys. Chem. Chem. Phys.*, 2000, **2**, 195; (*c*) L. Li, C. L. Fisher, R. Konecny, D. Bashford and L. Noodleman, *Inorg. Chem.*, 1999, **38**, 929; (*d*) J. Li, M. R. Nelson, C. Y. Peng, D. Bashford and L. Noodleman, *J. Phys Chem. A*, 1998, **102**, 6311; (*e*) S. A. Macgregor and K. K. Moock, *Inorg. Chem.*, 1998, **37**, 3284.
33 M.-H. Baik, C. K. Schauer and T. Ziegler, *J. Am. Chem. Soc.*, 2002, **124**, 11167.
34 H. Reiss and A. Heller, *J. Phys Chem.*, 1985, **89**, 4207.
35 K. Nagata, N. Takeda and N. Tokito, *Angew. Chem. Int. Ed. Engl.*, 2002, **41**, 136.
36 (*a*) J. G. Brennan, T. Siegrist, S. M. Stuczynski and M. L. Steigerwald, *J. Am. Chem. Soc.*, 1990, **112**, 9233; (*b*) R. D. Adams, T. A. Wolfe, B. W. Eichhorn and R. C. Haushalter, *Polyhedron*, 1989, **8**, 701; (*c*) H. Wolkers, K. Dehnicke, D. Fenske, A. Khassanov and S. S. Hafner, *Acta Crystallogr., Sect. C*, 1991, **47**, 1627.